Hindawi
Journal of Nanomaterials
Volume 2022, Article ID 3621807, 12 pages
https://doi.org/10.1155/2022/3621807

Research Article

Removal of Reactive Red 120 in a Batch Technique Using Seaweed-Based Biochar: A Response Surface Methodology Approach

Gokulan Ravindiran,[1] **Kalyani Gaddam**,[2] **and Killi Sunil**[3]

[1]*Department of Civil Engineering, GMR Institute of Technology, Rajam, Andhra Pradesh 532 127, India*
[2]*Department of Civil Engineering, Nadimpalli Satyanarayana Raju Institute of Technology, Visakhapatnam, Andhra Pradesh 531173, India*
[3]*Department of Chemical Engineering, College of Engineering and Technology, Samara University, Afar, Ethiopia 7240*

Correspondence should be addressed to Killi Sunil; sunilkilli@su.edu.et

Received 27 April 2022; Accepted 6 May 2022; Published 19 May 2022

Academic Editor: Samson Jerold Samuel Chelladurai

The elimination of Reactive Red 120 (RR120) from synthetic solution using biochar generated from *Ulva prolifera* was investigated. The process parameters sorbent dose (A), pH (B), initial dye concentration (C), and temperatures (D) were optimized using response surface methodology (RSM). To estimate the removal effectiveness of dye with the best 27 trails, the Box-Behnken method (blocked) was utilised. Analysis of variance (ANOVA), main effect plot, interaction plot, and surface plot were used to establish the significance of the model, and the confidence level of the model was set at 95%. To maximise the objective, the RSM optimizer was utilised with a desirability of 1. Furthermore, the batch investigation was supplemented by isotherm models, kinetic models, and thermodynamic analyses to understand the adsorption mechanism.

1. Introduction

Water is the primary source of survival for humans and aquatic life, and it has recently become a big concern. Many chemicals are introduced into water bodies as a result of home and industrial activities, resulting in water pollution [1]. Dyes cause significant water contamination. There are currently about 10,000 different types of dyes available in the industry [2]. Over the last three decades, the use of dyes in the textile, paint, paper and pulp, and leather sectors has steadily increased. Dyes are classified into two types: natural dyes and synthetic dyes. Natural dyes have various drawbacks, including limited availability, dyeing processing time, and expense. Synthetic dyes are created by colouring naturally occurring dyes. Dyes are further subdivided into reactive dyes, acid dyes, and cationic dyes [3]. Reactive dyes have various distinct properties. Reactive dyes will strongly bond to the cloth through the production of covalent bonds, resulting in good colouring over the fabric.

Ion exchange, membrane filtration, sedimentation, electrocoagulation, and chemical precipitation are some of the various treatment methods for separating contaminants from the effluent [4]. These traditional processes are time-consuming, and the colour treatment costs a lot of money. The adsorption technique is used to eliminate several hazardous contaminants. The key advantage of the adsorption method is that it takes less time and has a lower treatment cost, and regeneration of the sorbent will result in a lower overall treatment cost [5]. Activated carbon is one of the most common sorbents used in industry. Because of the heterogeneous nature of the activated carbon, a wide range of contaminants was absorbed [6]. Many researchers advocated the biosorption approach to solve the shortcomings of activated carbon. Biosorption is a method that uses either live or dead biomass to remove contaminants [7]. Many sorbents derived from waste leaf compost, neem seeds, tamarind seeds, industrial sludge, date seeds, orange peels, powdered nut shell, and rice husk have proven to be effective.

Table 1: Design of experiment input factors with different levels.

Levels			Variables	Code
1	0	-1		
1	2	3	Biochar dose (g/L)	A
2	3	4	pH	B
250	500	750	Initial dye concentration (mg/L)	C
30	35	40	Temperature (°C)	D

Table 2: Comparison of RSM and experimental removal efficiency with residual errors.

Run order	A	B	C	D	Efficiency (%)		Residual error
					Experimental	RSM predicted	
1	3	3	500	30	77.65	77.68	0.03
2	3	4	500	35	72.85	72.30	-0.55
3	2	3	500	35	77.10	76.06	-1.04
4	2	4	750	35	68.50	68.25	-0.25
5	2	3	750	30	73.30	73.72	0.42
6	1	3	500	30	67.15	66.96	-0.19
7	2	4	250	35	73.53	73.36	-0.16
8	1	2	500	35	71.23	71.99	0.76
9	2	3	750	40	73.75	74.05	0.30
10	2	3	250	30	78.33	78.23	-0.09
11	2	2	500	30	78.70	78.56	-0.14
12	2	2	750	35	75.40	75.29	-0.11
13	2	3	500	35	78.12	78.10	-0.02
14	3	2	500	35	79.75	79.16	-0.59
15	2	2	250	35	81.62	81.60	-0.02
16	1	3	750	35	63.85	63.10	-0.75
17	3	3	750	35	74.35	74.74	0.39
18	1	4	500	35	63.50	64.30	0.80
19	1	3	250	35	68.88	68.55	-0.33
20	2	4	500	40	72.25	72.45	0.20
21	2	3	500	35	79.20	80.26	1.06
22	1	3	500	40	67.60	67.30	-0.30
23	2	2	500	40	79.85	79.95	0.10
24	2	4	500	30	71.80	71.77	-0.03
25	3	3	250	35	81.23	82.04	0.81
26	3	3	500	40	78.10	78.01	-0.09
27	2	3	250	40	78.78	78.57	-0.21

Biochar is a new sorbent created through the pyrolysis process in an oxygen-limited environment [8]. Because of its improved properties, biochar has a high potential for harmful pollutant sorption. Because of the pyrolysis process, biochar is rich in carbon and has improved functional groups. Heavy metals and colour molecules are removed from effluents using biochar [9]. The spent biochar is then utilised to enhance the soil. In recent years, biochar has been seen as an environmental management tool capable of mitigating environmental concerns [10]. There are numerous approaches for improving the properties of biochar. Heat treatment, acid treatment, alkaline treatment, and the addition of foreign material to biochar result in the creation of a new unique biomaterial [11, 12].

RSM is a statistical tool for optimizing process conditions [13]. To obtain a single output-dependent variable, several input parameters are examined at various levels (response). The Box-Behnken approach is used to develop the design of tests, and it has intervals between -1 and +1, with the design predicting in-between values. RSM will reduce the number of trials required to obtain the output

Table 3: ANOVA for the developed model.

Source	DF	Adj SS	Adj MS	*F* value	*p* value	Remarks
Model	14	693.639	49.546	96.16	<0.001	Significant
Linear	4	572.566	143.141	277.80	<0.001	Significant
A	1	317.498	317.498	616.19	<0.001	Significant
B	1	162.251	162.251	314.89	<0.001	Significant
C	1	91.853	91.853	178.27	<0.001	Significant
D	1	0.963	0.963	1.87	0.197	—
Square	4	119.561	29.890	58.01	<0.001	Significant
A ∗ A	1	114.505	114.505	222.23	<0.001	Significant
B ∗ B	1	16.870	16.870	32.74	<0.001	Significant
C ∗ C	1	11.414	11.414	22.15	<0.001	Significant
D ∗ D	1	2.954	2.954	5.73	0.034	—
2-way interaction	6	1.512	0.252	0.49	0.805	—
A ∗ B	1	0.172	0.172	0.33	0.574	—
A ∗ C	1	0.860	0.860	1.67	0.221	—
A ∗ D	1	0.000	0.000	0.00	1.000	—
B ∗ C	1	0.357	0.357	0.69	0.421	—
B ∗ D	1	0.123	0.123	0.24	0.635	—
C ∗ D	1	0.000	0.000	0.00	1.000	—
Error	12	6.183	0.515	—	—	—
Lack-of-fit	10	3.978	0.398	0.36	0.890	—
Pure error	2	2.206	1.103	—	—	—
Total	26	699.822	—	—	—	—

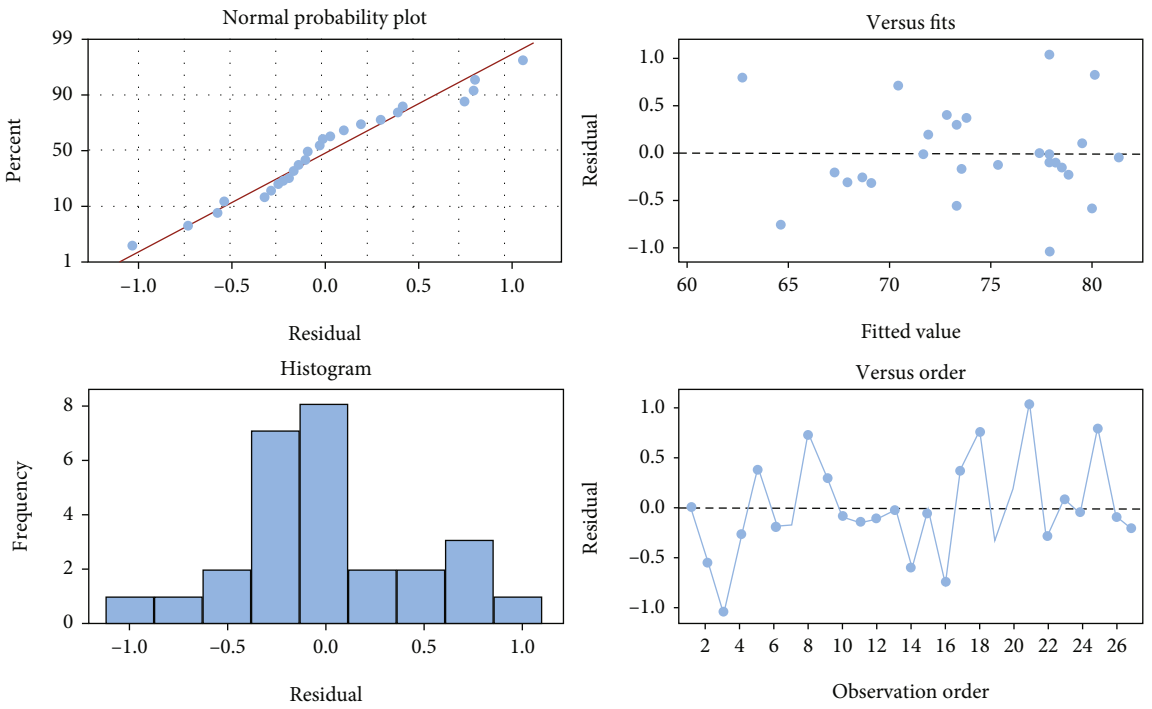

Figure 1: Probability plot for the observation of different trails.

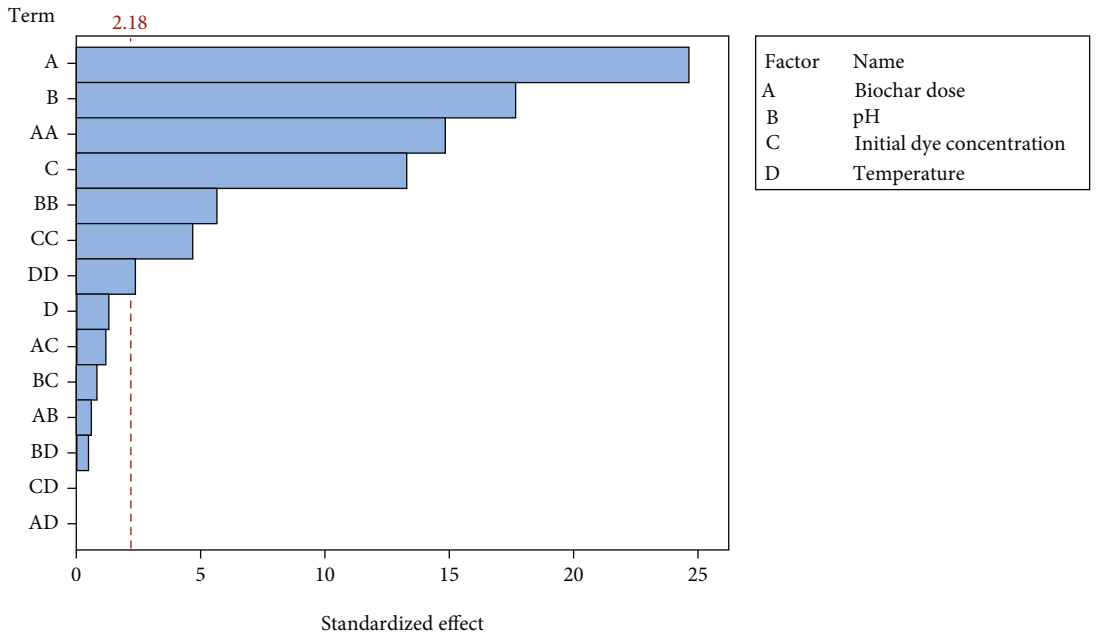

Figure 2: Pareto chart for different variables and their significance.

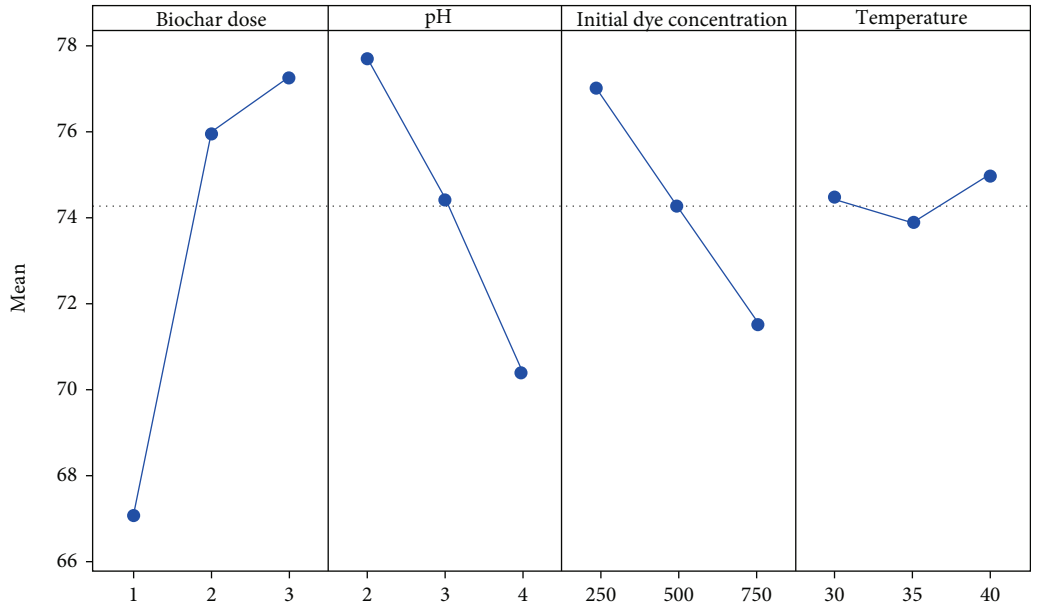

Figure 3: Main effect plot of different variables for responses.

[14, 15]. The current work employed 27 experimental trails based on four input variables to predict one output variable (biochar removal efficiency) for dye molecules. *Ulva prolifera* is widely available throughout the world's coastal regions. Because these marine seaweeds are naturally occurring, they can be obtained at a very low or no cost. The use of overgrown biomass as an environmental mitigation method for eutrophication in water bodies will be beneficial to the environment. Many experts believe *Ulva prolifera* biochar can be beneficial in the sorption of heavy metals, antibiotics, and other harmful substances [16]. The current work investigated the RR120 adsorption mechanism in a single solute system using various influencing parameters.

2. Materials and Methods

2.1. Biochar Preparation and Batch Adsorption Studies. The biochar was created using the biomass of *Ulva prolifera*. A preliminary treatment of the biomass was performed prior to the synthesis of biochar. Deionized water was

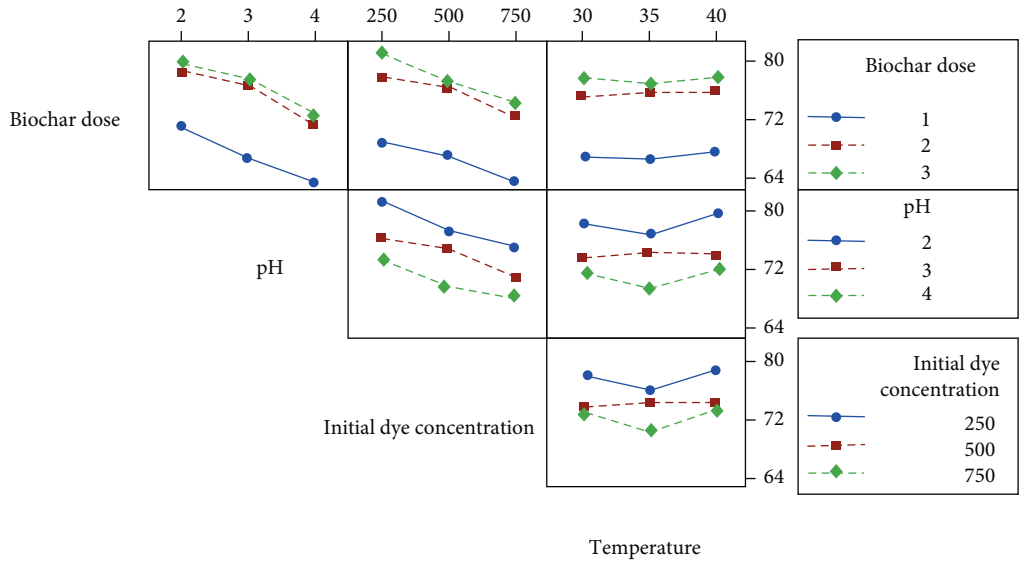

Figure 4: Interaction plot of different variables for the response (removal efficiency).

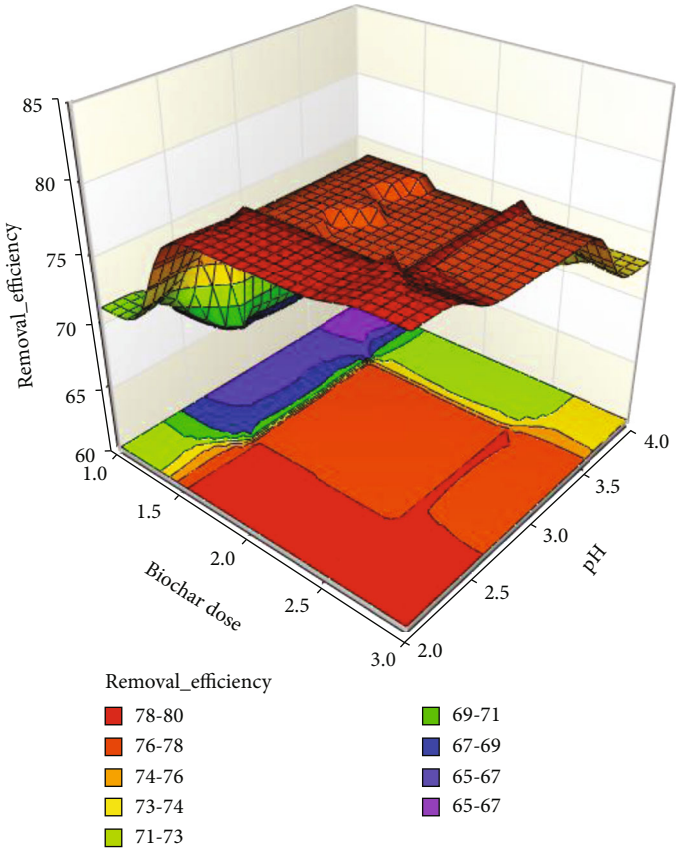

Figure 5: Surface plot: biochar (a) vs. pH (b).

used to eliminate dust particles and other contaminants (three times). To achieve a uniform size, the washed biomass was naturally dried and shredded into 7.5 mm pieces. To ensure the absence of moisture content, the shredded biomass was heated to 103°C. Finally, the dried biomass was placed in a muffle furnace to produce biochar. To begin, the muffle furnace was cleaned using nitrogen gas to verify that there was no oxygen present. The necessary amount of dried biomass was preserved in the crucible, which was then covered with aluminium

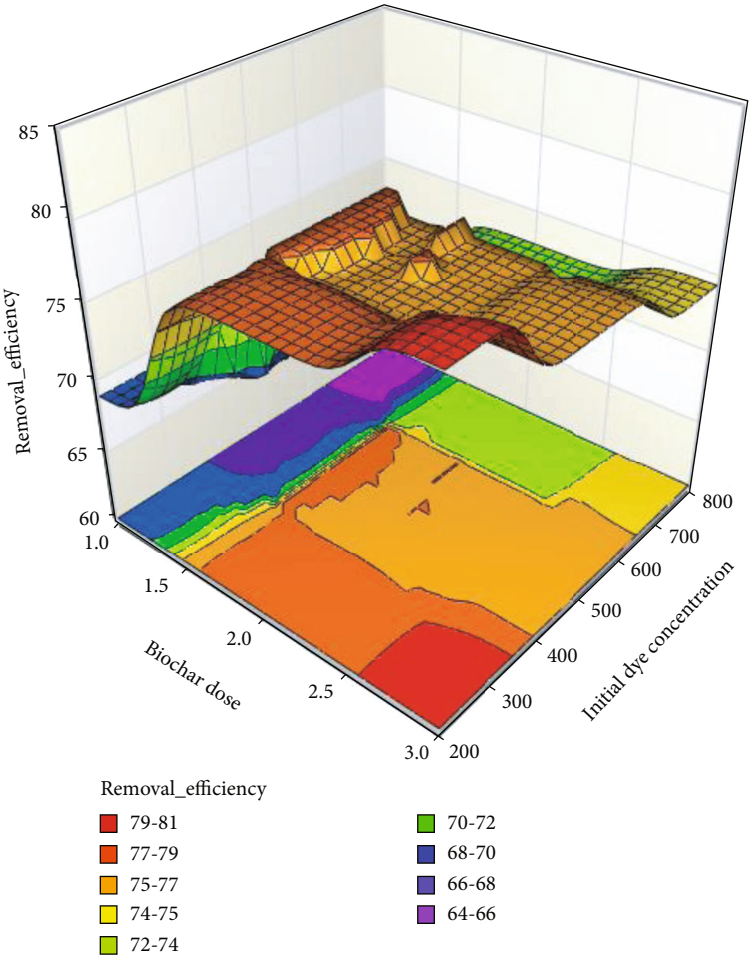

Figure 6: Surface plot: biochar (a) vs. initial dye concentration (c).

foil and pierced with two small holes. The pyrolysis temperature was held at 300°C for three hours, and the biochar was retained in the furnace until it reached room temperature. The batch adsorption study was carried out in the same manner as described in our prior research [17].

2.2. Response Surface Methodology. RSM used Minitab to create a Box-Behnken study design. The batch technique takes into account the biochar dosage (A), pH (B), initial RR120 concentration (C), and temperature (D) as input parameters. Table 1 summarises the variable's various levels.

3. Result and Discussion

3.1. Batch Adsorption Studies. The biochar dose (1 to 10 g/L), pH (1.75 to 5), initial dye concentration (100 to 1000 g/L), and temperature (20 to 45°C) were all varied in real-time batch tests. At ideal conditions, the batch adsorption results showed that 79.8 percent of the colour was removed [17]. The batch results came to the following conclusions. The removal effectiveness increased with an increase in biochar dose, initial dye concentration, and temperature but decreased with an increase in pH. The isotherm model determined that the Langmuir model best fit the experimental data with the highest correlation coefficient. The Langmuir isotherm indicates that the sorption was caused via chemisorption. Because of the accessibility of uniform binding sites, the results determined that the sorption of the dye molecules over the surface of the sorbent was even with single layers (monolayer adsorption). Between the adsorbate and the adsorbent, a strong equilibrium condition was achieved. The kinetic study is carried out to assess the sorption process at different time intervals with a constant initial dye concentration. The kinetic investigation indicated that the results predicted by the pseudo-second-order kinetic model are superior to the results predicted by the pseudo-first-order kinetic model, and the correlation coefficient for the PSO model was also good. PSO models fit only when the sorption was caused by a chemisorption mechanism. The thermodynamic analysis determined that the reactions are spontaneous and endothermic. The free energy value grew as the temperature rose. The negative Gibbs free energy and positive enthalpy values found that at high temperatures, reactions are spontaneous The

adsorbate and adsorbent's randomness is represented by the positive entropy value. Furthermore, the desorption studies validated the biochar's ability to sequentially adsorb and desorb for three cycles [17].

3.2. RSM-Design of Experiments. Equation (1) shows the model equation produced by the Box-Behnken approach for determining removal efficiency. The model was built using the linear, two-way interaction, and quadratic form of the various components. Table 2 shows the anticipated and experimental elimination efficiency of the 27 trails. The correlation value (R^2) was found to be 0.9912, indicating an excellent match for the model [18]. The adjusted correlation coefficient (adj R^2) was calculated to be 0.9902, with just a 0.01 difference between R^2 and adj R^2 [19]. The adj R^2 is used to determine the variance of the mean created by the model, and a small difference indicates that the model is significant.

$$\begin{aligned}\text{Removal Efficiency} = {} & 3.1 + 23.98\,\text{A} + 7.21\,\text{B} + 0.0125\,\text{C} \\ & + 2.245\,\text{D} - 4.634\,\text{A} * \text{A} - 1.779\,\text{B} * \text{B} \\ & - 0.000023\,\text{C} * \text{C} - 0.0298\,\text{D} * \text{D} \\ & + 0.208\,\text{A} * \text{B} - 0.00185\,\text{A} * \text{C} \\ & + 0.0000\,\text{A} * \text{D} + 0.00119\,\text{B} * \text{C} \\ & - 0.0350\,\text{B} * \text{D}.\end{aligned} \tag{1}$$

The results of the analysis of variance are reported in Table 3. The p and F values were used to determine the model significance for linear, quadratic, and two-way interactions of distinct components. The model assumes a 95 percent confidence level, and a p value of less than 0.05 indicates that the model is significant [20]. The p values of numerous components in Table 3 were less than 0.001, indicating that the model was significant. Temperature has a p value of 0.197, which is not statistically significant. The nonsignificance was due to the interaction of other factors with temperature and the quadratic shape of temperature. The higher the F value, the better the model. The relevance of a model is shown by a F value of 96.17 [21].

Figure 1 shows a normal probability map that can be used to determine if the distribution of expected values is normal or not. If the developed model is a good fit, the normalcy probability plot should stay close to a straight line. Many points are close to the expected normal probability plot, while those points away from the reference line are termed outliers, as seen in Figure 1. Fitted vs. residual values are compared, with fitted values on the x-axis and residual values on the y. The results show that the fits are unevenly spread out with fanning, implying that the variables are not constant. The order vs. residual method was used to determine if the data obtained had any residual. The results are inconsistent and unrelated to one another, and there is no clear justification for the residuals for each element. The amount of orders categorised concerning the error was often analysed using a histogram. According to the results, eight observations have an error between 0.1 and -0.1, and this histogram shows that approximately one-third of the data have insignificant errors, indicating the model's quality.

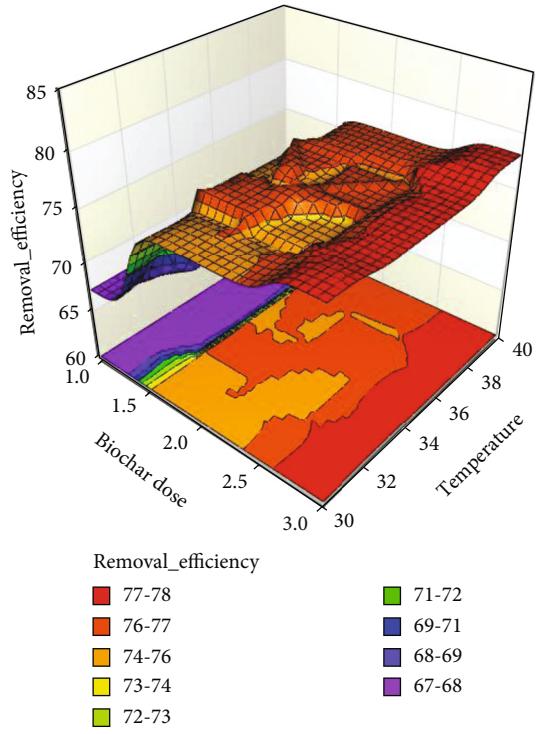

Figure 7: Surface plot: biochar (a) vs. temperature (d).

Figure 2 shows the Pareto chart for several factors. The Pareto chart creates a standard line to identify the variables that have a substantial impact on the answer. From the largest to the smallest effect, a Pareto chart is used to determine the standardised effect of all variables. The statistically significant level is indicated by the reference line, which is based on the significant level. The significance threshold is usually kept at 95 percent, or 0.05, which means the results are 95 percent correct. The importance is indicated by the individual and interaction factors crossing the reference line at 2.18. Factors and interactions that do not pass the 2.18 reference line are not significant. With the created models, the factors representing the bars at A, B, C, AA, BB, and CC suggest that these factors are important with a 95 percent accuracy. Temperature was not a statistically significant factor. For D and DD, the coded coefficient of the p value was 0.197 and 0.34, respectively. To be considered significant, the p value must be less than 0.05. The p value for all remaining temperature interactions was more than 0.05 and not significant. Temperature and the interaction of other parameters with temperature are not significant for the created model, according to the Pareto chart.

3.3. Main Effect and Interaction Plot of Variables. The major effect plot of all factors was depicted in Figure 3. The results showed that removal efficiency improved with

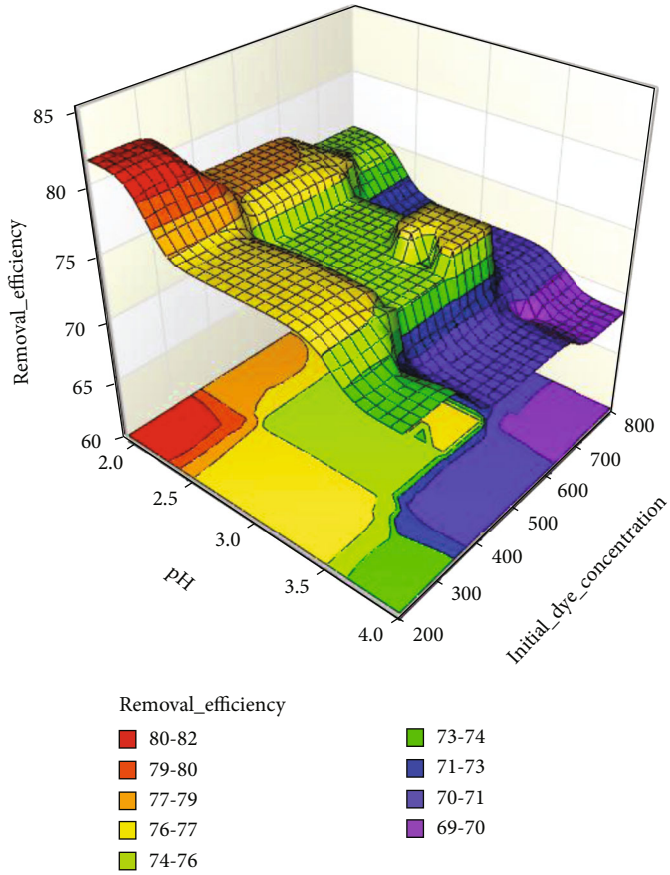

Figure 8: Surface plot: pH (b) vs. initial dye concentration (c).

increasing biochar dose, decreased with increasing pH, and decreased with increasing dye concentration. The temperature dropped at first, but a subsequent rise in temperature increased the removal efficiency. Biochar with a larger dosage may have more binding sites for the colour molecules available. The pH determines the effectiveness of elimination. The biochar's point of zero charges was found to be 6.72. At a pH of 6.72, the available positive and negative charges on the surface are neutral. Positive charges develop more quickly in pH changes less than a point of zero change, while negative charges develop more quickly in pH changes higher than a point of zero change [22]. Because reactive dyes are negatively charged ions, sorption will increase when pH is reduced. This could lead to superior elimination efficiency at pH 2 rather than pH 4. The initial dye concentration indicates how many dye molecules are accessible to bind to available binding sites. A higher dosage may have resulted in more dye molecules being deposited at the binding sites [23]. Temperature is thought to be a significant influencing factor in the sorption process. Initially, increasing the temperature from 30 to 35°C reduced the removal efficiency, but increasing the temperature from 35 to 40°C improved the efficiency. It implies that sorption can take place as a result of physical or chemical adsorption.

The interaction pot for many variables is depicted in Figure 4. The continuous response (removal efficiency) to the first- and second-category components is determined using an interaction plot. The outcomes of interaction plots can be parallel or nonparallel lines. There was no interaction between the variables, as indicated by the parallel line. The nonparallel line implies that there is a lot of interaction between the variables. Figure 4 depicts the nonparallel lines, which proved that the variables had a substantial interaction. The following conclusions can be drawn from the graph, for example. When biochar is the first factor, a dose of 3 g/L of biochar produced the best results with all other interacting variables. At 2, 250 mg/L, and 40°C, the secondary parameters pH (B), initial dye concentration (C), and temperature (D) showed the best responses. When pH was taken into account as the initial consideration, a pH of 2 produced the best results. At 3, 250 mg/L, and 40°C, the secondary variables of biochar, initial dye concentration, and temperature showed maximal responses. So, based on the interaction plot, $A = 3$ g/L, $B = 2$, $C = 250$ mg/L, and $D = 40$°C were determined to be the best conditions for maximal response yield.

3.4. Surface Plot of Different Variables. The surface plot is used to visualise the relationship between two independent variables and the desired result. Surface plots usually

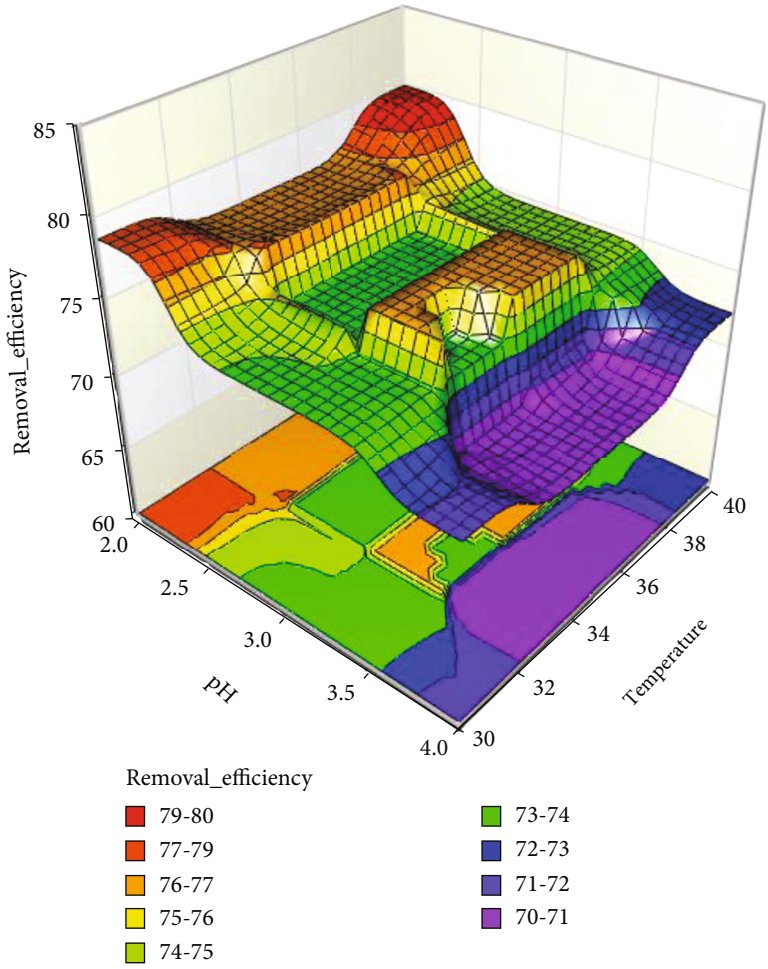

Figure 9: Surface plot: pH (b) vs. temperature (d).

include three axes: X, Y, and Z. The X- and Z-axes are used to input independent variables, while the Y-axis is used to display desired replies. Figures 5–10 show how different variables interact to get a desired response (removal efficiency). Figure 5 shows the X- and Z-axes as the biochar dose and pH, respectively. The removal efficiency is allocated to the Y-axis. The surface plot of these two parameters revealed that a pH of 2 to 2.5 and a biochar dose of 1.5 to 3 g/L resulted in the highest removal effectiveness of 78-80 percent. It was also determined that an increase in pH and a decrease in biochar dose both reduced efficiency. From the surface plot, it can be deduced that a lower pH and a higher biochar dose are required for maximum removal effectiveness. The surface contact between biochar dosage and initial dye concentration was depicted in Figure 6. With a biochar dose of 2.5 to 3 g/L and an initial dye concentration of 200 to 300 mg/L, a removal efficiency of 79 to 81 percent was achieved. The surface plot of temperature vs. biochar dose is shown in Figure 7. Between a biochar dose of 2.5 to 3 and a temperature of 35 to 40°C, a maximum removal effectiveness of 78 to 79 percent was achieved. The surface plot between pH and initial dye concentration is shown in Figure 8. When the pH was kept between 2 and 2.5 and the initial dye concentration was 200 to 300 mg/L, the removal efficiency was 80 to 82 percent. At a pH of 2 and a temperature of 40°C, Figure 9 depicts the surface interaction between pH and temperature, with an efficiency of 79 to 80 percent. The surface interactions of initial dye concentration and temperature are depicted in Figure 10. With a dye concentration of 200 to 300 mg/L and a temperature of 35 to 40°C, a removal efficiency of 78 to 79 percent was achieved.

3.5. RSM Optimizer. The optimization plot is used to increase the range of selected elements with a high attractiveness level or to maximise the response. The goal of this study was to boost responsiveness by taking into account all aspects at a desired level of 1. Setting the goal to maximise the reaction enhanced the response. The actual lower and higher responses were 63.5 and 81.62 percent, respectively. At process circumstances of A of 2.5 g/L, B of 2, C of 250 mg/L, and D of 36.5°C, the composite desirability of 1 was attained, with a response of 83.28 percent. Using the RSM optimization plot, a progressive increase of 1.66 percent was obtained. A boundary layer was created by varying

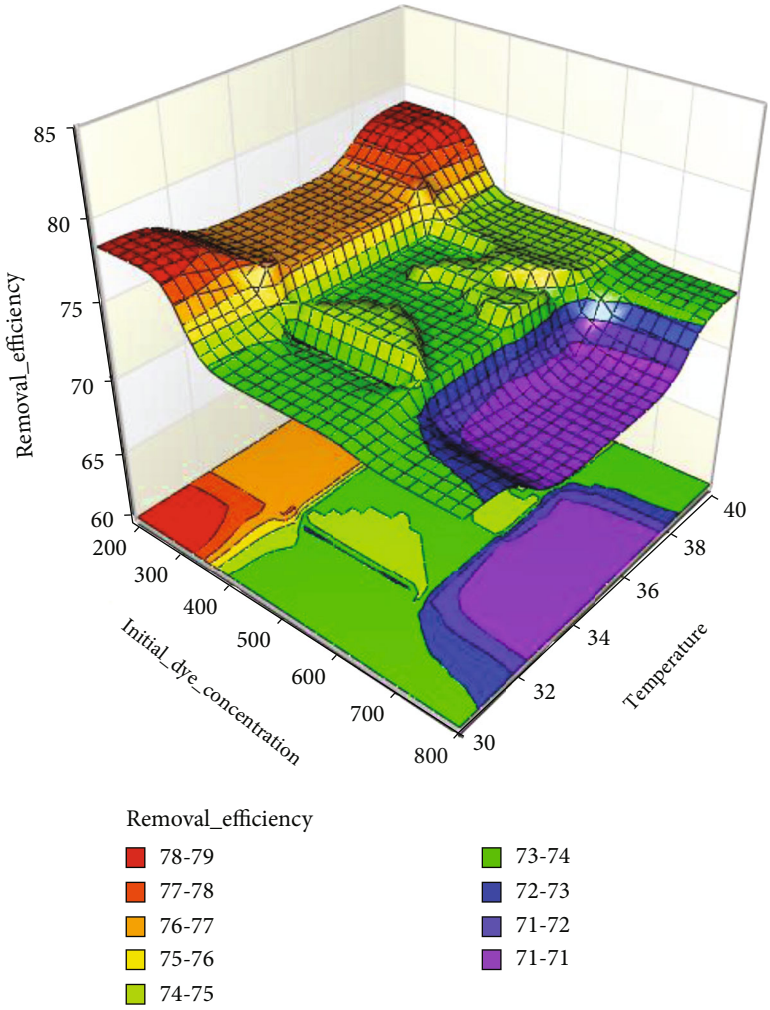

Figure 10: Surface plot: initial dye concentration (c) vs. temperature (d).

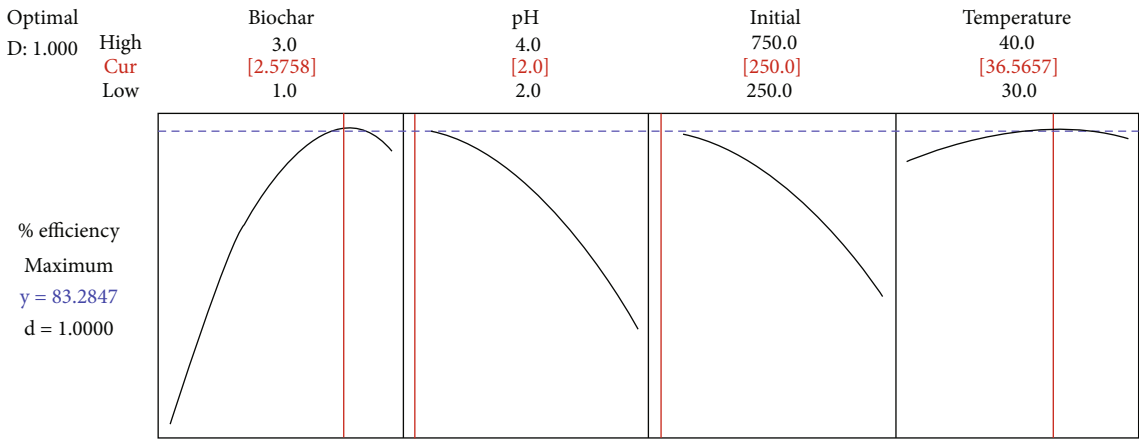

Figure 11: RSM optimization plot.

the prediction interval (PI) between 81.16 and 85.40. To have a significant model, the RSM optimal predictor must fall inside this range. An optimization graphic was used to establish the process conditions for a batch experiment. Three sets of trials were carried out, resulting in an average removal efficiency of 82.90 percent. The RSM optimization plot for the reactive red 120 elimination is shown in Figure 11.

4. Conclusion

The following conclusions were reached as a result of the current inquiry.

(i) The chemisorption method was responsible for the sorption of reactive red 120 employing *Ulva prolifera*

(ii) Thermodynamic tests demonstrated that the reactions are endothermic and spontaneous

(iii) Using the response surface approach, the maximum removal efficiency was determined to be 81.62 percent

(iv) The major effect plot revealed that as pH and initial dye concentration increased, removal efficiency declined, whereas it increased as biochar dose and temperature increased

(v) RSM's optimization plot revealed that by adjusting the parameters, a removal effectiveness of 83.28 percent may be achieved

Data Availability

The data used to support the findings of this study are included in the article.

Disclosure

This research was carried out as part of Samara University's employment in Ethiopia.

Conflicts of Interest

The authors declare that they have no conflicts of interest.

Acknowledgments

The authors are grateful to Samara University in Ethiopia for their assistance. The authors appreciate the support and encouragement they received from the GMR Institute of Technology in Rajam and Nadimpalli Satyanarayana Raju Institute of Technology in Visakhapatnam.

References

[1] A. Abdolali, W. S. Guo, H. H. Ngo, S. S. Chen, N. C. Nguyen, and K. L. Tung, "Typical lignocellulosic wastes and by-products for biosorption process in water and wastewater treatment: a critical review," *Bioresource Technology*, vol. 160, pp. 57–66, 2014.

[2] T. S. Anirudhan and M. Ramachandran, "Adsorptive removal of basic dyes from aqueous solutions by surfactant modified bentonite clay (organoclay): kinetic and competitive adsorption isotherm," *Process Safety and Environment Protection*, vol. 95, pp. 215–225, 2015.

[3] A. Fegousse, A. El Gaidoumi, Y. Miyah, R. El Mountassir, and A. Lahrichi, "Pineapple bark performance in dyes adsorption: optimization by the central composite design," *Journal of Chemotherapy*, vol. 2019, article 3017163, pp. 1–11, 2019.

[4] A. S. Franca, L. S. Oliveira, and M. E. Ferreira, "Kinetics and equilibrium studies of methylene blue adsorption by spent coffee grounds," *Desalination*, vol. 249, no. 1, pp. 267–272, 2009.

[5] M. T. Yagub, T. K. Sen, S. Afroze, and H. M. Ang, "Dye and its removal from aqueous solution by adsorption: a review," *Advances in Colloid and Interface Science*, vol. 209, pp. 172–184, 2014.

[6] A. M. Ferreira, J. A. P. Coutinho, A. M. Fernandes, and M. G. Freire, "Complete removal of textile dyes from aqueous media using ionic-liquid-based aqueous two-phase systems," *Separation and Purification Technology*, vol. 128, pp. 58–66, 2014.

[7] N. Gupta, A. K. Kushwaha, and M. C. Chattopadhyaya, "Application of potato (Solanum tuberosum) plant wastes for the removal of methylene blue and malachite green dye from aqueous solution," *Arabian Journal of Chemistry*, vol. 9, pp. S707–S716, 2016.

[8] T. A. Saleh and V. K. Gupta, "Photo-catalyzed degradation of hazardous dye methyl orange by use of a composite catalyst consisting of multi-walled carbon nanotubes and titanium dioxide," *Journal of Colloid and Interface Science*, vol. 371, no. 1, pp. 101–106, 2012.

[9] D. S. Kharat, "Preparing agricultural residue-based adsorbents for removal of dyes from effluents - a review," *Brazilian Journal of Chemical Engineering*, vol. 32, no. 1, pp. 1–12, 2015.

[10] J. Lehmann and S. Joseph, "Biochar for environmental management: an introduction," in *Biochar for Environmental Management: Science and Technology*, pp. 1–12, Science and Technology. Earthscan, London, 2009.

[11] Y. Liu and Y. J. Liu, "Biosorption isotherms, kinetics and thermodynamics," *Separation and Purification Technology*, vol. 61, no. 3, pp. 229–242, 2008.

[12] L. Beesley, E. Moreno-Jiménez, J. L. Gomez-Eyles, E. Harris, B. Robinson, and T. Sizmur, "A review of biochars' potential role in the remediation, revegetation and restoration of contaminated soils," *Environmental Pollution*, vol. 159, no. 12, pp. 3269–3282, 2011.

[13] M. G. Moghaddam and M. Khajeh, "Comparison of response surface methodology and artificial neural network in predicting the microwave-assisted extraction procedure to determine zinc in fish muscles," *Food and Nutrition Sciences*, vol. 2, no. 8, pp. 803–808, 2011.

[14] N. Isoda, R. Rodrigues, A. Silva et al., "Optimization of preparation conditions of activated carbon from agriculture waste utilizing factorial design," *Powder Technology*, vol. 256, pp. 175–181, 2014.

[15] A. Deb, A. Debnath, and B. Saha, "Ultrasound-aided rapid and enhanced adsorption of anionic dyes from binary dye matrix onto novel hematite/polyaniline nanocomposite: response surface methodology optimization," *Applied Organometallic Chemistry*, vol. 34, no. 2, 2020.

[16] A. Robic, C. Rondeau-Mouro, J. F. Sassi, Y. Lerat, and M. Lahaye, "Structure and interactions of ulvan in the cell wall of the marine green algae Ulva rotundata (Ulvales, Chlorophyceae)," *Carbohydrate Polymers*, vol. 77, no. 2, pp. 206–216, 2009.

[17] S. Mahendran, R. Gokulan, A. Aravindan et al., "Production of *Ulva Prolifera* derived biochar and evaluation of adsorptive removal of reactive red 120: batch, isotherm, kinetic, thermodynamic and regeneration studies," *Biomass Conversion and Biorefinery*, pp. 1–12, 2021.

[18] J. Jaafari and K. Yaghmaeian, "Response surface methodological approach for optimizing heavy metal biosorption by the blue-green alga Chroococcus disperses," *Desalination and Water Treatment*, vol. 142, pp. 225–234, 2019.

[19] H. Mazaheri, M. Ghaedi, M. H. Ahmadi Azqhandi, and A. Asfaram, "Application of machine/statistical learning, artificial intelligence and statistical experimental design for the modeling and optimization of methylene blue and Cd(ii) removal from a binary aqueous solution by natural walnut carbon," *Physical Chemistry Chemical Physics*, vol. 19, no. 18, pp. 11299–11317, 2017.

[20] G. Sodeifian, S. A. Sajadian, and N. SaadatiArdestani, "Evaluation of the response surface and hybrid artificial neural network- genetic algorithm methodologies to determine extraction yield of Ferulago angulata through supercritical fluid," *Journal of the Taiwan Institute of Chemical Engineers*, vol. 60, pp. 165–173, 2016.

[21] M. L. Sundar, G. Kalyani, R. Gokulan, S. Ragunath, and H. Joga Rao, "Comparative adsorptive removal of reactive red 120 using RSM and ANFIS models in batch and packed bed column," *Biomass Conversion and Biorefinery*, pp. 1–17, 2021.

[22] K. Vijayaraghavan and Y. S. Yun, "Competition of reactive red 4, reactive orange 16 and basic blue 3 during biosorption of reactive blue 4 by polysulfone-immobilized Corynebacterium glutamicum," *Journal of Hazardous Materials*, vol. 153, no. 1-2, pp. 478–486, 2008.

[23] Z. Aksu and Ş. Ş. Çağatay, "Investigation of biosorption of Gemazol Turquise Blue-G reactive dye by dried Rhizopus arrhizus in batch and continuous systems," *Separation and Purification Technology*, vol. 48, no. 1, pp. 24–35, 2006.